On the stability analysis of a pair of van der Pol oscillators with delayed self-connection, position and velocity couplings

Cite as: AIP Advances **3**, 112118 (2013); https://doi.org/10.1063/1.4834115
Submitted: 24 April 2013 • Accepted: 30 October 2013 • Published Online: 20 November 2013

Kun Hu and Kwok-wai Chung

On the stability analysis of a pair of van der Pol oscillators with delayed self-connection, position and velocity couplings

Kun Hu[1,2] and Kwok-wai Chung[2,a]
[1]*School of Mathematics and Computational Science, Sun Yat-sen University, Guangzhou, 510275, P.R.China*
[2]*Department of Mathematics, City University of Hong Kong, 83 Tat Chee Avenue, Kowloon, Hong Kong*

(Received 24 April 2013; accepted 30 October 2013; published online 20 November 2013)

In this paper, we perform a stability analysis of a pair of van der Pol oscillators with delayed self-connection, position and velocity couplings. Bifurcation diagram of the damping, position and velocity coupling strengths is constructed, which gives insight into how stability boundary curves come into existence and how these curves evolve from small closed loops into open-ended curves. The van der Pol oscillator has been considered by many researchers as the nodes for various networks. It is inherently unstable at the zero equilibrium. Stability control of a network is always an important problem. Currently, the stabilization of the zero equilibrium of a pair of van der Pol oscillators can be achieved only for small damping strength by using delayed velocity coupling. An interesting question arises naturally: can the zero equilibrium be stabilized for an arbitrarily large value of the damping strength? We prove that it can be. In addition, a simple condition is given on how to choose the feedback parameters to achieve such goal. We further investigate how the in-phase mode or the out-of-phase mode of a periodic solution is related to the stability boundary curve that it emerges from a Hopf bifurcation. Analytical expression of a periodic solution is derived using an integration method. Some illustrative examples show that the theoretical prediction and numerical simulation are in good agreement. [http://dx.doi.org/10.1063/1.4834115]

I. INTRODUCTION

Many important physical, chemical and biological systems such as semiconductor lasers,[1,2] coupled Brusselator models[3,4] and neural networks for circadian pacemakers[5] are composed of coupled nonlinear oscillators. Ubiquitous in nature due to finite propagation speeds of signals, time delay may have profound effects on the collective dynamics of such systems. The study of the effects of time delay on the collective states has received much attention in recent years.[6–9] In particular, the van der Pol oscillator has been considered by many researchers as the nodes for various networks. Atay[10] investigated the effect of delayed feedback for the van der Pol oscillator on oscillatory behavior. Maccari[11] investigated the resonance of a parametrically excited van der Pol oscillator under state feedback control with a time delay. From the viewpoint of vibration control, they demonstrated that the time delay and the feedback pairs could enhance the control performance and reduce the amplitude peak. For a van der Pol-Duffing oscillator with delayed position feedback, Xu and Chung[12] showed that time delay might be used as a simple but efficient switch to control motions of a system: either from orderly motion to chaos or from chaotic motion to order for different applications. Wirkus and Rand[13] studied the dynamics of two weakly coupled van der Pol oscillators

[a]Electronic mail: makchung@cityu.edu.hk

with delayed velocity coupling due to its relevance to coupled laser oscillators. They found that both the in-phase and out-of-phase modes were stable for delays of about a quarter of the uncoupled period of the oscillators. Li *et al.*[14] extended the above work by including both delayed position and velocity coupling. They showed that, for the case of 1:1 internal resonance, both the in-phase mode and out-of-phase mode existed when the two coupling coefficients were identical, and there were two death domains when these two modes did not exist. Zhang and Gu[15] considered the dynamics of a system of two van der Pol equations with delay position coupling. They showed the existence of stability switches and, as the delay is varied, a sequence of Hopf bifurcations occurred at the zero equilibrium. Song[16] investigated the stability switches of two van der Pol oscillators with delay velocity coupling, and obtained different in-phase and anti-phase patterns as the coupling delay was increased. In the above papers, only weakly nonlinear van der Pol oscillators were investigated.

One of the most interesting and important collective behaviors in coupled oscillators that have aroused much attention in recent years is the amplitude death which refers to the diffusive-coupling-induced stabilization of unstable fixed points in coupled oscillators.[17,18] The theoretical and practical meanings of the phenomenon of amplitude death in coupled systems are of great significance. For example, it is a desirable control mechanism in cases such as coupled lasers where it leads to stabilization[19,20] and a pathological case of oscillation suppression or disruption in cases like neuronal disorders such as Alzheimers disease, Parkinsons disease, etc.[21–25] For the occurrence of amplitude death, one of the following conditions is needed: the parameter mismatch,[18,26] the time-delayed coupling,[27] dynamical coupling[28] and conjugate coupling.[29] Amplitude death by delay was first reported by Ramana Reddy *et al.*[27] in their study of a pair of limit cycle oscillators which were the normal form for the Hopf bifurcation. A novel result[30] that they found was the occurrence of amplitude death even in the absence of a frequency mismatch between the two oscillators. Based on the system studied in Ref. 30, Song *et al.*[31] gave more detailed and specific conditions on the existence of amplitude death for different delays. Since Pyragas[32] introduced a novel feedback control method of using a single time delay some two decades ago, the investigation has been extended to multiple time delays[33] for stabilizing steady states of various chaotic dynamical systems. For several well-known chaotic systems, Ahlborn and Parlitz[34] showed that multiple delay feedback control is more effective for fixed point stabilization in terms of stability and flexibility, in particular for large delay times. Blyuss *et al.*[35] applied delayed feedback control to stabilize an unstable steady state of a neutral delay differential equation. They showed that a number of amplitude death regions came into existence in the parameter space due to the interplay between the control strength and two time delays. For the van der Pol-Duffing system with delayed position feedback, Xu *et al.*[36] obtained an amplitude death region near a weak resonant double Hopf bifurcation point. A thorough review of the current works can be found in Ref. 37.

The effect of time delay on the amplitude death of the Stuart-Landau oscillators with linearly (diffusively) delay coupling has been well studied.[27,37] As for the van der Pol oscillators with delay coupling, investigations have been focused only on the weakly nonlinear situation. For the pair of van der Pol oscillators with delay velocity coupling studied in Ref. 16, amplitude death is possible only when the damping strength is less than 0.5. Complex dynamics such as periodic-doubling sequences leading to chaos occur for strongly nonlinear situation.[38] An interesting question naturally arises: can the strongly nonlinear van der Pol oscillators be stabilized using delay coupling? In other words, is it possible to derive a delay feedback control strategy such that amplitude death exists for all positive values of the damping strength? Ahlborn and Parlitz[34] suggested that more delays entering into the control terms were more effective and flexible for fixed point stabilization. Due to the complicated analytical expressions, the analysis of systems with multiple delays is always based on numerical simulations. It would be invaluable to develop an efficient analytical method for problems with multiple delays. Delayed position and velocity feedbacks are two kinds of strategies commonly used for control purposes. However, there are very few investigations on using both kinds for the stability control of the van der Pol oscillators. These situations constitute the motivation of the present paper.

In this paper, our goal is to derive a delay feedback control strategy for the amplitude death of nonlinear van der Pol oscillators with arbitrary large damping strength and investigate periodic solutions of the in-phase and out-of-phase modes arising from Hopf bifurcation. In doing so, we introduce three kinds of feedbacks namely, position, velocity, self-connection and three time

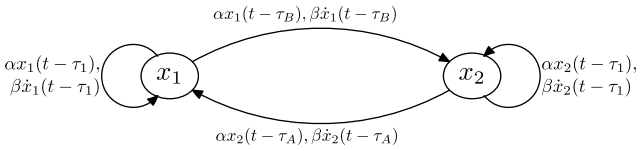

FIG. 1. A pair of van der Pol oscillators with discrete time delays in the signal transmission of self-connection, position and velocity couplings.

delays. The paper is organized as follows. Sec. II describes the model formulation and introduces a parameter γ for finding the solutions of the characteristic equation of the linearized system. Local stability analysis of the zero equilibrium is preformed in Sec. III. Bifurcation diagram of the system parameters is constructed and the properties of the stability boundary curves in the plane of time delays are discussed. In Sec. IV, we turn our attention to amplitude death region in the plane of time delays and prove a sufficient condition for its existence for arbitrary large damping strength. Sec. V is devoted to the investigation of the periodic solutions of the in-phase and the out-of-phase modes. We show how the type of mode is related to the stability boundary curves obtained in Sec. III. An integration method is employed to study the amplitude of periodic solutions arising from a Hopf bifurcation. As illustrated in Sec. VI, the analytical results are in good agreement with those obtained from numerical simulations. Finally, Sec. VII contains the conclusions.

II. MODEL FORMULATION

We study a pair of van der Pol oscillators in which there are distinct, discrete time delays in the signal transmission of self-connection, position and velocity couplings. The coupled system is shown schematically in Fig. 1 and expressed in two delay differential equations as

$$\begin{aligned}
&\ddot{x}_1(t) + \mu[x_1^2(t) - 1]\dot{x}_1(t) + x_1(t) \\
&\quad = \alpha[x_2(t-\tau_A) - x_1(t-\tau_1)] + \beta[\dot{x}_2(t-\tau_A) - \dot{x}_1(t-\tau_1)], \\
&\ddot{x}_2(t) + \mu[x_2^2(t) - 1]\dot{x}_2(t) + x_2(t) \\
&\quad = \alpha[x_1(t-\tau_B) - x_2(t-\tau_1)] + \beta[\dot{x}_1(t-\tau_B)) - \dot{x}_2(t-\tau_1)].
\end{aligned} \tag{1}$$

where τ_1, τ_A and τ_B are, respectively, the time delays of self-connection, from oscillator x_2 to x_1, and from x_1 to x_2; α and β are, respectively, the position and velocity coupling strengths; μ is the damping strength which is always positive. Let $y_1(t) = \dot{x}_1(t)$ and $y_2(t) = \dot{x}_2(t)$, system (1) can be written as

$$\begin{aligned}
\dot{x}_1(t) &= y_1(t), \\
\dot{y}_1(t) &= -x_1(t) - \mu[x_1^2(t) - 1]y_1(t) \\
&\quad + \alpha[x_2(t-\tau_A) - x_1(t-\tau_1)] + \beta[y_2(t-\tau_A) - y_1(t-\tau_1)], \\
\dot{x}_2(t) &= y_2(t), \\
\dot{y}_2(t) &= -x_2(t) - \mu[x_2^2(t) - 1]y_2(t) \\
&\quad + \alpha[x_1(t-\tau_B) - x_2(t-\tau_1)] + \beta[y_1(t-\tau_B) - y_2(t-\tau_1)].
\end{aligned} \tag{2}$$

We note that system (2) is reduced to the system investigated in Ref. 15 if $\beta = \tau_1 = 0$ and that of Ref. 16 if $\alpha = \tau_1 = 0$. The characteristic equation of the linearization of system (2) at the origin is given by

$$\Delta(\lambda, \tau_1, \tau_2) = \Delta_1(\lambda, \tau_1, \tau_2)\Delta_2(\lambda, \tau_1, \tau_2) = 0, \tag{3a}$$

where $\tau_2 = \frac{\tau_A + \tau_B}{2}$ and

$$\Delta_1(\lambda, \tau_1, \tau_2) = \lambda^2 - \mu\lambda + 1 + (\beta\lambda + \alpha)(e^{-\lambda\tau_1} - e^{-\lambda\tau_2}), \tag{3b}$$

$$\Delta_2(\lambda, \tau_1, \tau_2) = \lambda^2 - \mu\lambda + 1 + (\beta\lambda + \alpha)(e^{-\lambda\tau_1} + e^{-\lambda\tau_2}). \tag{3c}$$

Equation (3a) determines the local stability of the origin in (1). When $\tau_1 = \tau_2 = 0$, (3a) has the following four roots:

$$\lambda_{1,2} = \frac{1}{2}(\mu \pm \sqrt{\mu^2 - 4}), \quad \text{and} \quad \lambda_{3,4} = \frac{1}{2}\mu - \beta \pm \sqrt{\left(\frac{\mu}{2} - \beta\right)^2 - (1 + 2\alpha)}. \tag{3d}$$

Since $\mu > 0$, the origin is always unstable. To investigate the distribution of roots of (3a) for nonzero τ_1 and τ_2, we have to consider the stability boundary curves of (3b) and (3c) by letting $\lambda = i\omega$ for $\omega > 0$. From (3b) and (3c), we obtain, respectively,

$$\cos(\omega\tau_2) = \cos(\omega\tau_1) - \frac{A}{\beta^2\omega^2 + \alpha^2}, \quad \sin(\omega\tau_2) = \sin(\omega\tau_1) - \frac{B}{\beta^2\omega^2 + \alpha^2}, \tag{4a}$$

and

$$\cos(\omega\tau_2) = \frac{A}{\beta^2\omega^2 + \alpha^2} - \cos(\omega\tau_1), \quad \sin(\omega\tau_2) = \frac{B}{\beta^2\omega^2 + \alpha^2} - \sin(\omega\tau_1), \tag{4b}$$

where $A = (\mu\beta + \alpha)\omega^2 - \alpha$ and $B = \omega(\beta\omega^2 - \mu\alpha - \beta)$. Eliminating τ_2 in (4a) or (4b), we arrive at the same equation

$$\omega^4 + (\mu^2 - 2)\omega^2 + 1 - 2A\cos(\omega\tau_1) - 2B\sin(\omega\tau_1) = 0. \tag{5}$$

Let $C = \sqrt{A^2 + B^2} = \sqrt{(\beta^2\omega^2 + \alpha^2)[\omega^4 + (\mu^2 - 2)\omega^2 + 1]}$, and

$$\sin\theta = \frac{A}{C} \quad \text{and} \quad \cos\theta = \frac{B}{C}. \tag{6}$$

Then, after simplification, (5) becomes

$$\sqrt{\omega^4 + (\mu^2 - 2)\omega^2 + 1} = 2\sqrt{\beta^2\omega^2 + \alpha^2}\gamma, \quad \text{where} \quad \gamma = \sin(\theta + \omega\tau_1). \tag{7}$$

It follows from (7) that $0 < \gamma \leq 1$. Substituting (6) and (7) into (4a), we obtain

$$\cos\omega\tau_2 = \cos\omega\tau_1 - 2\gamma\sin\theta, \quad \sin\omega\tau_2 = \sin\omega\tau_1 - 2\gamma\cos\theta,$$

$$\Longrightarrow \tau_2 = \frac{2n\pi - 2\theta}{\omega} - \tau_1, \quad \text{for } n \in \mathbb{Z}. \tag{8}$$

To simplify the subsequent calculations, we let $\alpha = k\beta$. It follows from (7) and (8) that $\Delta_1(i\omega, \tau_1, \tau_2) = 0$ in (3b) is equivalent to

$$\omega^4 + (\mu^2 - 2 - 4\beta^2\gamma^2)\omega^2 + 1 - 4k^2\beta^2\gamma^2 = 0, \tag{9a}$$

$$\gamma = \sin(\theta + \omega\tau_1) \in (0, 1], \tag{9b}$$

$$\tau_2 = \frac{2n\pi - 2\theta}{\omega} - \tau_1, \quad \text{for } n \in \mathbb{Z}. \tag{9c}$$

Similarly, $\Delta_2(i\omega, \tau_1, \tau_2) = 0$ in (3c) is equivalent to

$$\omega^4 + (\mu^2 - 2 - 4\beta^2\gamma^2)\omega^2 + 1 - 4k^2\beta^2\gamma^2 = 0, \tag{10a}$$

$$\gamma = \sin(\theta + \omega\tau_1) \in (0, 1], \tag{10b}$$

$$\tau_2 = \frac{(2n+1)\pi - 2\theta}{\omega} - \tau_1, \quad \text{for } n \in \mathbb{Z}. \tag{10c}$$

For the solutions of (3b), we may first choose $\gamma \in (0, 1]$ and obtain ω if it exists from (9a). Then, τ_1 and τ_2 can be obtained from (9b) and (9c), respectively.

III. LOCAL STABILITY ANALYSIS

In this section, we investigate the number of positive solutions of ω in (3a) and construct bifurcation diagram in the parameter space of μ, β and k. The van der Pol oscillator is inherently unstable at the zero equilibrium. A study of positive solution of ω gives the condition of μ, β and k that a pair of eigenvalues of (3a) cross the imaginary axis, resulting in a change of stability at the zero equilibrium. For a given k, we will show that the bifurcation diagram (μ, β) is partitioned into three regions according to whether the stability boundary curves exist (closed or open-ended) or not. For a region with no positive solution, the zero equilibrium is always unstable even when delays exist. The existence of two positive solutions in a region may lead to the occurrence of amplitude death, i.e. the stabilization of the zero equilibrium.

Let $\Gamma = (\mu^2 - 2 - 4\beta^2\gamma^2)^2 - 4(1 - 4k^2\beta^2\gamma^2)$ be the discriminant of (9a). Since (9a) is a quadratic equation in ω^2, we have the following lemma regarding the number of positive roots of ω in (9a).

Lemma 1. *Let $k, \beta \in \mathbb{R}$, $\mu \in \mathbb{R}^+$, $\gamma \in (0, 1]$ and assume*
(B_1) either $\mu^2 - 2 - 4\beta^2\gamma^2 \geq 0$ and $1 - 4k^2\beta^2\gamma^2 > 0$ or $\Gamma < 0$;
(B_2) either $1 - 4k^2\beta^2\gamma^2 < 0$, or $\mu^2 - 2 - 4\beta^2\gamma^2 < 0$ and $\Gamma = 0$;
(B_3) $\mu^2 - 2 - 4\beta^2\gamma^2 < 0$, $1 - 4k^2\beta^2\gamma^2 > 0$ and $\Gamma > 0$.
Then, $(B_1) - (B_3)$ are the conditions for 0, 1 and 2 positive real roots, respectively, of ω in (9a).

To investigate how Γ varies with respect to $\mu > 0$ and k, we consider the equation $\Gamma = 0$ and obtain

$$\gamma^4 + \frac{1}{\beta^2}\left(k^2 + 1 - \frac{\mu^2}{2}\right)\gamma^2 + \frac{\mu^2(\mu^2 - 4)}{16\beta^4} = 0 \tag{11a}$$

$$\Longrightarrow \gamma_\pm^2 = \frac{1}{2\beta^2}\left[\frac{\mu^2}{2} - 1 - k^2 \pm \sqrt{(1 + k^2)^2 - \mu^2 k^2}\right]. \tag{11b}$$

With some calculations on inequalities, we obtain the regions in the (k, μ) plane with 0, 1 and 2 positive real roots of γ in (11a) as follows:

Lemma 2. *Let $k \in \mathbb{R}$, $\mu \in \mathbb{R}^+$ and assume*
(C_1) either $|k| \geq 1$ and $\mu > 2$, or $\mu > \frac{1+k^2}{|k|}$;
(C_2) either $\mu < 2$, or $|k| < 1$ and $\mu = \frac{1+k^2}{|k|}$;
(C_3) $|k| < 1$ and $2 < \mu < \frac{1+k^2}{|k|}$.
Then, $(C_1) - (C_3)$ are the conditions for 0, 1 and 2 positive real roots, respectively, of γ in (11a) (see Fig. 2).

Remark 1 The curve segment $\mu = \frac{1+k^2}{|k|}$ with $|k| < 1$, which is the boundary of (C_1) and (C_3), belongs to (C_2).

Remark 2 For given $\mu > 0$, k and if (11a) has a positive real root in γ, there exists β such that $\gamma \in (0, 1]$.

Next, we consider the bifurcation diagram of (9a) with respect to the number of positive roots in ω for $\gamma \in (0, 1]$. Define

$$\gamma_1 = \frac{1}{2|k\beta|} > 0 \quad \text{and} \quad \gamma_2^2 = \frac{\mu^2 - 2}{4\beta^2}, \tag{12}$$

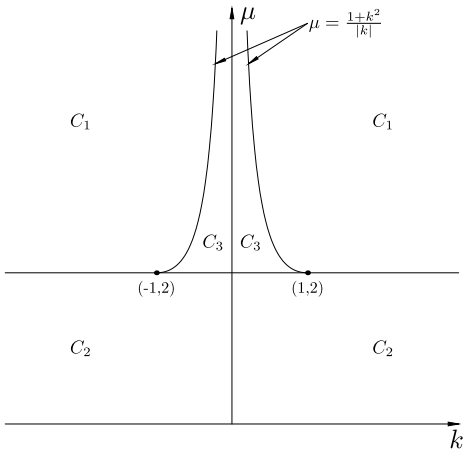

FIG. 2. Number of positive roots of γ in (11a). There are 0, 1 and 2 positive real roots in regions C_1, C_2 and C_3, respectively. The curve segment $(k, \frac{1+k^2}{|k|})$ with $|k| < 1$ belongs to (C_2).

so that $1 - 4k^2\beta^2\gamma_1^2 = 0$ and $\mu^2 - 2 - 4\beta^2\gamma_2^2 = 0$, respectively. Since $\gamma_1 > 1 \Leftrightarrow |\beta| < \frac{1}{2|k|}$ and together with Lemmas 1 and 2, we have the following conditions of γ_1, γ_2 and γ_+ (which is defined in (11b)) on the number of positive roots of ω in (9a):

Lemma 3. *Assume that $\gamma_1 > 1$. Then, for $\gamma \in (0, 1]$,*
(a) if $\gamma_2^2 \geq 1$ or $\gamma_+ > 1$, (9a) has no positive solution;
(b) if $\gamma_2^2 < 1$ and $\gamma_+ \leq 1$, (9a) has 0, 1 or 2 positive solutions according to $\gamma < \gamma_+$, $\gamma = \gamma_+$ or $\gamma_+ < \gamma \leq 1$, respectively.

Lemma 4. *Assume that $\gamma_1 \leq 1$. Then, for $\gamma \in (0, 1]$,*
(a) if $\gamma_1^2 \leq \gamma_2^2$, (9a) has 0 or 1 positive solution according to $\gamma \leq \gamma_1$ or $\gamma_1 < \gamma \leq 1$, respectively;
(b) if $\gamma_1^2 > \gamma_2^2$, (9a) has 0, 1, 2 or 1 positive solution accordng to $\gamma < \gamma_+$, $\gamma = \gamma_+$, $\gamma_+ < \gamma < \gamma_1$ or $\gamma_1 \leq \gamma \leq 1$, respectively.

For $\gamma \in (0, 1]$, we define $\gamma = \sin c$ for $0 < c \leq \frac{\pi}{2}$. Then, for a positive solution of (9a), (τ_1, τ_2) in (9b) and (9c) can be expressed as

$$(\tau_1, \tau_2) = \left(\frac{2m\pi + c - \theta}{\omega}, \frac{2m_1\pi - c - \theta}{\omega} \right), \tag{13a}$$

or

$$(\tau_1, \tau_2) = \left(\frac{(2m+1)\pi - c - \theta}{\omega}, \frac{(2m_1 - 1)\pi + c - \theta}{\omega} \right), \tag{13b}$$

where m, $m_1 = m - n \geq 0$. Since (10a) is the same as (9a) and for a positive solution of (10a), (τ_1, τ_2) in (10b) and (10c) is given by

$$(\tau_1, \tau_2) = \left(\frac{2m\pi + c - \theta}{\omega}, \frac{(2m_1 + 1)\pi - c - \theta}{\omega} \right), \tag{13c}$$

or

$$(\tau_1, \tau_2) = \left(\frac{(2m+1)\pi - c - \theta}{\omega}, \frac{2m_1\pi + c - \theta}{\omega} \right). \tag{13d}$$

In the above consideration, we use γ as a parameter to find the purely imaginary roots of (3a). The following theorem gives the bifurcation diagram of (3a) with respect to the number of purely imaginary roots.

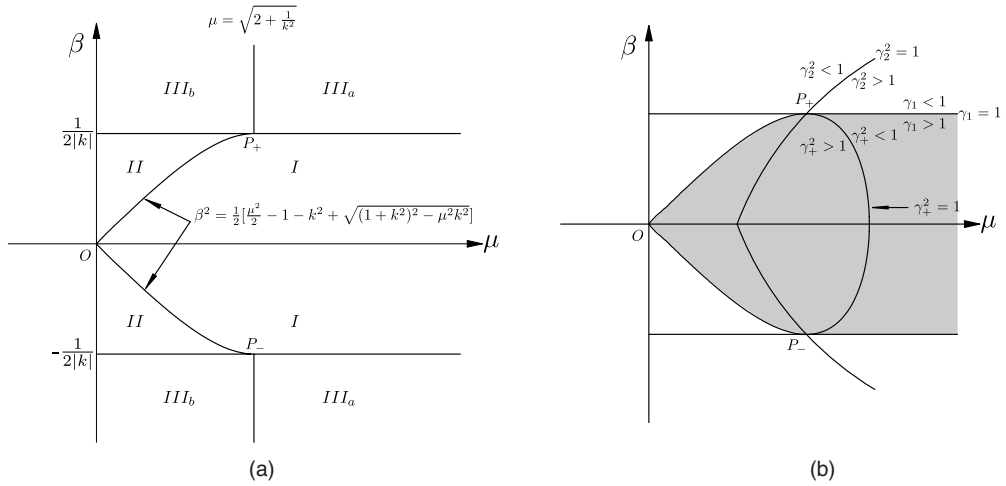

FIG. 3. (a) Bifurcation diagram of (3a) with respect to the number of purely imaginary roots; (b) Curves of $\gamma_i^2 = 1$ for $i \in \{+, 1, 2\}$ and regions where γ_i^2 is greater/less than one. These curves intersect concurrently at $P_\pm = (\sqrt{2+\frac{1}{k^2}}, \pm\frac{1}{2|k|})$.

Theorem 1. *Let $k, \beta \in \mathbb{R}$, $\mu \in \mathbb{R}^+$ and define the following regions in the (μ, β) plane as*

$$(\textit{region I}): \begin{cases} \beta^2 < \frac{1}{2}\left[\frac{\mu^2}{2} - 1 - k^2 + \sqrt{(1+k^2)^2 - \mu^2 k^2}\right], & \textit{for } \mu < \sqrt{2+\frac{1}{k^2}}, \\ |\beta| < \frac{1}{2|k|}, & \textit{for } \mu \geq \sqrt{2+\frac{1}{k^2}}; \end{cases}$$

$(\textit{region II})$: $|\beta| < \frac{1}{2|k|}$, $\mu < \sqrt{2+\frac{1}{k^2}}$ *and* $\beta^2 \geq \frac{1}{2}\left[\frac{\mu^2}{2} - 1 - k^2 + \sqrt{(1+k^2)^2 - \mu^2 k^2}\right]$;

$(\textit{region III}_a)$: $|\beta| \geq \frac{1}{2|k|}$ *and* $\mu \geq \sqrt{2+\frac{1}{k^2}}$;

$(\textit{region III}_b)$: $|\beta| \geq \frac{1}{2|k|}$ *and* $\mu < \sqrt{2+\frac{1}{k^2}}$.

(*see Fig. 3 for the above regions.*)

(*a*) *If k, β and μ satisfy the condition of region I, then (3a) has no purely imaginary root.*

(*b*) *If k, β and μ satisfy the condition of region II, then (3a) has 0, 1 or 2 pairs of purely imaginary roots according to $\gamma < \gamma_+$, $\gamma = \gamma_+$ or $\gamma_+ < \gamma \leq 1$, respectively.*

(*c*) *If k, β and μ satisfy the condition of region III_a, then (3a) has 0 or 1 pair of purely imaginary roots according to $\gamma \leq \gamma_1$, or $\gamma_1 < \gamma \leq 1$, respectively.*

(*d*) *If k, β and μ satisfy the condition of region III_b, then (3a) has 0, 1, 2 or 1 pair of purely imaginary roots according to $\gamma < \gamma_+$, $\gamma = \gamma_+$, $\gamma_+ < \gamma < \gamma_1$ or $\gamma_1 \leq \gamma \leq 1$, respectively.*

Furthermore, given $\gamma \in (0, 1]$ and for $m, m_1 \geq 0$, the stability boundary curves in the (τ_1, τ_2) plane can be obtained from (13a)-(13d) for $\tau_1, \tau_2 > 0$.

Proof. See Appendix A. □

Theorem 1 provides information of and construction method for the stability boundary curves in the (τ_1, τ_2) plane.

Remark 1 For the values of k, β and μ in region *I*, since (3a) has no purely imaginary root, there is no stability boundary curve in the (τ_1, τ_2) plane. Therefore, both $\Delta(\lambda, \tau_1, \tau_2) = 0$ and $\Delta(\lambda, 0, 0) = 0$ have four roots in the right-half plane.

Remark 2 For the values of k, β and μ in region *II*, stability boundary curves can be constructed using (13a)-(13d) for $\gamma \in [\gamma_+, 1]$. Since ω is always finite and so do τ_1 and τ_2, the curves form closed loops which may intersect itself (see Fig. 4). When the values of μ, β and k tend to either OP_+ or OP_- such that $\gamma_+ = 1$, i.e. $c = \frac{\pi}{2}$, the loops shrink to the set of discrete points

$$(\tau_1, \tau_2) = \left(\frac{(2m + \frac{1}{2})\pi - \theta}{\omega}, \frac{(2m_1 \pm \frac{1}{2})\pi - \theta}{\omega}\right), \tag{14}$$

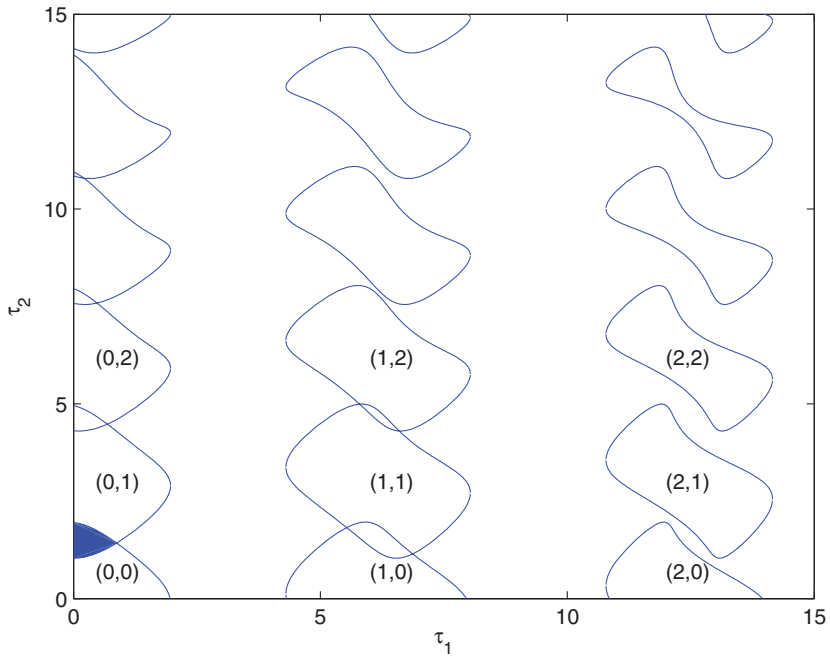

FIG. 4. Stability boundary curves in the (τ_1, τ_2) plane for $(\mu, k, \beta) = (0.05, 0.05, 0.1)$ (region II of Theorem 1). The ordered pair in a loop shows the values of (m, m_1) in (13a)-(13d). The overlapping areas are amplitude death regions.

where $m, m_1 \geq 0$ and $\tau_1, \tau_2 > 0$.

Remark 3 For the values of k, β and μ in regions III_a or III_b, one of the roots of (9a) vanishes at $\gamma = \gamma_1$. Then, both τ_1 and τ_2 in (13a)-(13d) become infinite. Therefore, the stability boundary curves are open-ended (see Fig. 5).

For the parameters of μ, β and k in region II, stability boundary loops in the (τ_1, τ_2) plane can be constructed in the following way:

(a) Set $\gamma = \gamma_+$ in (9a). From (9a) and (11b), $\omega = \omega_+$ is given by

$$\omega_+^2 = 1 + 2\beta^2\gamma_+^2 - \frac{\mu^2}{2} = \sqrt{(1+k^2)^2 - \mu^2 k^2} - k^2. \tag{15}$$

(b) Find the corresponding value of $\theta = \theta_+$ from (6) and $c = c_+$ where $\gamma_+ = \sin c_+$ with $0 < c_+ \leq \frac{\pi}{2}$.

(c) Segments from the pairs {(13a) and (13b)} and {(13c) and (13d)} form closed stability boundary loops as γ increases from γ_+ to 1.

From numerical simulation, we observe that two horizontally neighboring loops never intersect each other to form amplitude death region. However, it may occur to two vertically neighboring loops with small m and m_1(see Fig. 4). For $m = 0$, the small loops are initially born in the left-half (τ_1, τ_2) plane and, as $|\beta|$ increases, part of their interior crosses the τ_2-axis into the right-half (τ_1, τ_2) plane. In fact, in Fig. 4 where $\mu = 0.05$, (3a) has two pairs of eigenvalues in the right-half plane when (τ_1, τ_2) is outside the loops. Inside each loop (but not inside an overlapping area), (3a) has a pair of eigenvalues in the right-half plane. Inside the overlapping areas, all the eigenvalues of (3a) are in the left-half plane and thus these areas are amplitude death regions. To find the possibility of amplitude death region for arbitrary large μ, we investigate the intersection of stability boundary curves with $m = 0$ and the τ_2-axis.

We first find the value of β for which a stability boundary curve with $m = 0$ is tangential to τ_2-axis. When $\tau_1 = 0$, (5) is reduced to

$$\omega^4 + (\mu^2 - 2 - 2k\beta - 2\mu\beta)\omega^2 + 2k\beta + 1 = 0. \tag{16}$$

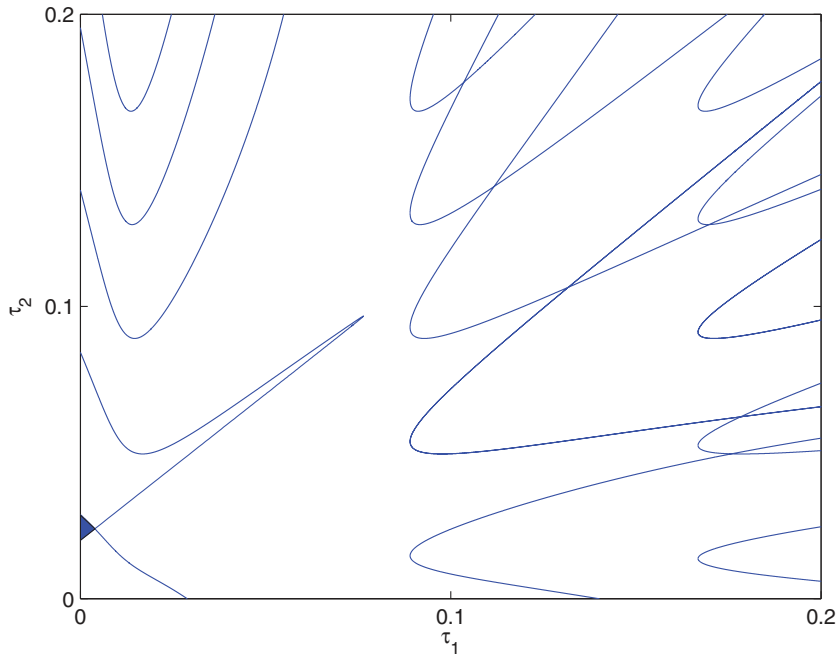

FIG. 5. Stability boundary curves in the (τ_1, τ_2) plane for $(\mu, k, \beta) = (20, 25, 40)$(region III of Theorem 1). The shaded area is an amplitude death region.

At a tangential point, (16) has a double root in ω^2 such that the discriminant vanishes, i.e.

$$(\mu + k)^2\beta^2 + \mu(2 - k\mu - \mu^2)\beta + \mu^2(\mu^2/4 - 1) = 0. \tag{17}$$

The larger root β_T of (17) and the double root of ω^2 in (16) are given by, respectively,

$$\beta_T = \frac{\mu(\mu^2 + k\mu - 2 + 2\sqrt{1 + k\mu + k^2})}{2(\mu + k)^2}, \tag{18}$$

and

$$\omega_T^2 = \frac{k + \mu\sqrt{1 + k\mu + k^2}}{\mu + k}. \tag{19}$$

In the stability control of the coupled van der Pol system for arbitrary large value of μ, we may assume that k is positive. At $\beta = \beta_T$, it follows from (4b) that

$$A = \beta_T[(\mu + k)\omega_T^2 - k] = \beta_T\mu\sqrt{1 + k\mu + k^2} > 0 \tag{20a}$$

and

$$\begin{aligned} B &= \omega_T\beta_T(\omega_T^2 - \mu k - 1) \\ &= \frac{-\omega_T\beta_T\mu\sqrt{1 + k\mu + k^2}(\sqrt{1 + k\mu + k^2} - 1)}{\mu + k} < 0. \end{aligned} \tag{20b}$$

Let $\theta = \theta_T$ at $\beta = \beta_T$. It follows from (6) that θ_T is in the second quadrant. Therefore, the tangential point is generated from (13b) or (13d) since $\pi/2 < \theta_T = \pi - c < \pi$. For $\beta > \beta_T$, (16) has two positive roots ω_1 and ω_2 where $\omega_1 < \omega_T < \omega_2$ and each stability boundary curve intersects the τ_2-axis at two points. From (13a)-(13d) with $\tau_1 = m = 0$, we denote the intersection points by

$$\tau_2^{(i,n)} = \frac{n\pi - 2\theta_i}{\omega_i} \quad \text{for} \quad i = 1, 2, n \geq 1, \tag{21}$$

and θ_i is obtained from (6) with $\omega = \omega_i$. For delay-coupled van der Pol oscillators with one delay, it was shown in Ref. 15 and 16 that stability switchings occur along the time-delay axis. For the generalized system (3a), we apply the results of Ref. 39 which studied the stability boundary curves of general linear systems with two delays. The following theorem states the directions of crossing the imaginary axis for solutions of $\Delta_i(\lambda, \tau_1, \tau_2) = 0\,(i = 1, 2)$ at these intersection points in the positive τ_2 direction.

Theorem 2. *Let* $\tau_2^{(i,n)}(i = 1, 2$ *and* $n \geq 1)$ *be defined in* (21) *and* $(0, \tau_2^{(i,n)})$ *be points generated by* (13a)-(13d) *with* $\tau_1 = m = 0$. *As* $(0, \tau_2)$ *crosses* $(0, \tau_2^{(1,n)})$ $((0, \tau_2^{(2,n)})$, *resp.*) *in the positive* τ_2 *direction, a pair of solutions of* $\Delta_i(\lambda, 0, \tau_2) = 0\,(i = 1, 2)$ *cross the imaginary axis to the left (right, resp.).*

Remark 1 From (20a) and (20b), θ_1 in (21) is always in the second quadrant. Therefore, from (21), $\tau_2^{(1,1)} < 0$ and $\tau_2^{(1,2)} > 0$.

Remark 2 When $\beta > \frac{\mu}{2}$, we have $\tau_2^{(2,1)} > 0$. Furthermore, $\Delta(\lambda, 0, 0) = 0$ in (3a) has only two roots with positive real parts, namely $\lambda_{1,2}$ in (3d). Among the intersection points on the positive τ_2-axis, either $(0, \tau_2^{(1,2)})$ or $(0, \tau_2^{(2,1)})$ is the nearest to the origin.

Remark 3 It follows from Theorem 2 that if

$$\beta > \frac{\mu}{2} \quad \text{and} \quad \tau_2^{(1,2)} < \tau_2^{(2,1)}, \tag{22}$$

all the roots of $\Delta(\lambda, 0, \tau_2) = 0$ have negative real part for $\tau_2 \in (\tau_2^{(1,2)}, \tau_2^{(2,1)})$. Thus, the interior of the intersection of the two stability boundary curves is an amplitude death region (see the shaded areas in Figs. 4 and 5).

IV. EXISTENCE OF AMPLITUDE DEATH REGION FOR ARBITRARY DAMPING STRENGTH

The system investigated in Ref. 16 is a special case of system (2) in that $\alpha = \tau_1 = 0$ and amplitude death is possible only when $\mu < 0.5$. By adding a position delay feedback (i.e. $\alpha \neq 0$) to the system in Ref. 16 while keeping $\tau_1 = 0$, is it possible to obtain amplitude death for arbitrary large $\mu > 0$? We give an affirmative answer.

To find sufficient conditions in terms of μ, k, β which satisfy the second condition in (22) we note that

$$\tau_2^{(1,2)} = \frac{2(\pi - \theta_1)}{\omega_1} < \frac{2\tan(\pi - \theta_1)}{\omega_1} \quad \text{and} \quad \frac{\pi - 2\tan\theta_2}{\omega_2} < \tau_2^{(2,1)} = \frac{\pi - 2\theta_2}{\omega_2}.$$

Given $\mu > 0$, the condition

$$\frac{2\tan(\pi - \theta_1)}{\omega_1} < \frac{\pi - 2\tan\theta_2}{\omega_2} \tag{23}$$

is sufficient for $\tau_2^{(1,2)} < \tau_2^{(2,1)}$. Substituting (6) into (23) and after simplification, we obtain the following sufficient condition for the existence of amplitude death region.

Theorem 3. *If* $k_1 = \frac{\beta}{\mu}$ *and* $k_2 = \frac{k}{\mu}$ *such that*

$$k_1 > \frac{1}{2} + \frac{8}{\pi^2}, \quad \textit{and} \quad [\pi k_1 k_2 (2k_1 - 1)]^2 > [2k_1(k_2 + 1) - 1]^3, \tag{24}$$

then the origin of system (2) *is stable for* $\tau_2 \in (\tau_2^{(1,2)}, \tau_2^{(2,1)})$.

In Fig. 6, the shaded region in the $(\frac{\beta}{\mu}, \frac{k}{\mu})$ plane satisfies (24). As an illustrative example, for arbitrary $\mu > 0$, we may choose $k_1 = \beta/\mu = 2$, $k_2 = k/\mu = 1.25$ and $\tau_2 = [\tau_2^{(1,2)} + \tau_2^{(2,1)}]/2$ so that the conditions in Theorem 3 are satisfied. For instance, when $\mu = 20$, we have $\beta = 40$, $k = 25$ and $\tau_2 = [\tau_2^{(1,2)} + \tau_2^{(2,1)}]/2 = (0.02 + 0.0288)/2 = 0.0244$. From numerical simulations,

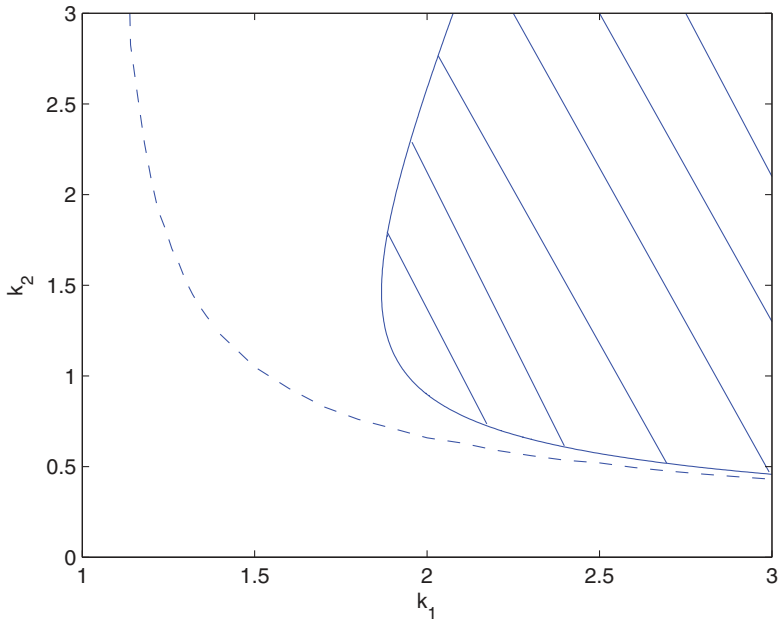

FIG. 6. Regions for the existence of amplitude death of system (1) in the (τ_1, τ_2) plane: the shaded region satisfies (24) in Theorem 3 whilst the region to the right of the dashed line satisfies condition (22).

Figs. 7(a)-7(b) show the time history of x_1 and x_2 in (1) without time delay (i.e. $\tau_1 = \tau_2 = 0$). As observed from the long-term behavior, a stable periodic solution exists. However, for $\tau_2^{(1,2)} < \tau_2 < \tau_2^{(2,1)}$, the zero equilibrium is asymptotically stable, as depicted in Figs. 7(c)-7(d) where $\tau_2 = 0.0244$.

Theorem 3 provides a sufficient condition for the existence of amplitude death region based on (23). To obtain a more accurate region in Fig. 6 for the existence of amplitude death region, we may use the second condition of (22) as

$$\tau_2^{(1,2)} = \frac{2(\pi - \theta_1)}{\omega_1} < \tau_2^{(2,1)} = \frac{\pi - 2\theta_2}{\omega_2} \tag{25}$$

For a given value of k_1, the minimum value of k_2 for which (25) is satisfied can be computed numerically. The region is also plotted in Fig. 6. The shaded region is inside the region to the right of the dashed curve since condition (23) is more conservative than (25). It is observed that the boundary curve from numerical result is asymptotically close to that of the second condition of (24) as $k_1 \to \infty$.

V. IN-PHASE/OUT-OF-PHASE MODES AND AN INTEGRATION METHOD

In the study of two weakly coupled van der Pol oscillators with delayed velocity coupling, Wirkus and Rand[13] found that both the in-phase and out-of-phase modes were stable for delays of about a quarter of the uncoupled period of the oscillators. In the bifurcation analysis of system (1) with delayed position and velocity couplings, we are going to investigate how the in-phase and out-of-phase modes occur and derive an analytical expression for a periodic solution arising from Hopf bifurcation using an integration method.

For simplicity, we assume in system (1) that $\tau_A = \tau_B = \tau_2$. We take τ_1 as the bifurcation parameter and assume a Hopf bifurcation occurs at $\tau_1 = \tau_{10}$. Other bifurcation parameter such as τ_2 can be treated in a similar way. For a small perturbation $\tau_1 = \tau_{10} + \epsilon\tau_{11}$, a periodic solution $z = (z_1, z_2)^T$ of order $\epsilon^{1/2}$ comes into existence. Let $z_i = \epsilon^{1/2} x_i$ for $i = 1, 2$. Since $z_{i,\tau_{10}+\epsilon\tau_{11}} = z_{i,\tau_{10}} - \epsilon\tau_{11}\dot{z}_{i,\tau_{10}}$ and $\dot{z}_{i,\tau_{10}+\epsilon\tau_{11}} = \dot{z}_{i,\tau_{10}} - \epsilon\tau_{11}\ddot{z}_{i,\tau_{10}}$ for $i = 1, 2$, (1) can be expressed in matrix form as

$$\ddot{z} - \mu\dot{z} + z + \alpha(z_{\tau_{10}} - Jz_{\tau_2}) + \beta(\dot{z}_{\tau_{10}} - J\dot{z}_{\tau_2}) = \epsilon f, \tag{26}$$

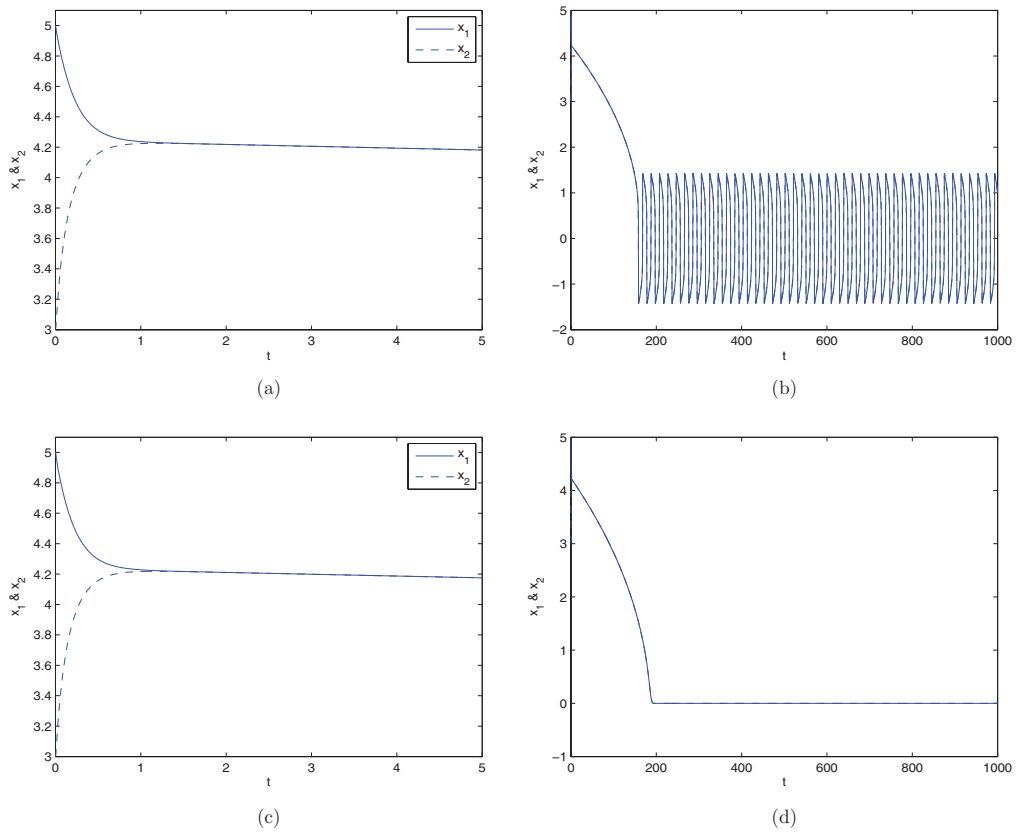

FIG. 7. Time history of (x_1, x_2) for $(\mu, k, \beta) = (20, 25, 40)$: (a) transient and (b) long-term behavior when $\tau_2 = 0$; and (c) transient behavior and (d) asymptotically stable when $\tau_2 = 0.0244$.

where $z = \begin{pmatrix} z_1 \\ z_2 \end{pmatrix}$, $z_{\tau_{10}} = \begin{pmatrix} z_{1,\tau_{10}} \\ z_{2,\tau_{10}} \end{pmatrix}$, $z_{\tau_2} = \begin{pmatrix} z_{1,\tau_2} \\ z_{2,\tau_2} \end{pmatrix}$, $J = \begin{pmatrix} 0 & 1 \\ 1 & 0 \end{pmatrix}$, and $f = \begin{pmatrix} -\mu z_1^2 \dot{z}_1 + \alpha\tau_{11}\dot{z}_{1,\tau_{10}} + \beta\tau_{11}\ddot{z}_{1,\tau_{10}} \\ -\mu z_2^2 \dot{z}_2 + \alpha\tau_{11}\dot{z}_{2,\tau_{10}} + \beta\tau_{11}\ddot{z}_{2,\tau_{10}} \end{pmatrix}$.

Theorem 4. *A periodic solution of (26) is of the in-phase mode (out-of-phase mode, resp.) if it emerges from a Hopf bifurcation on a stability boundary curve generated by (9a)–(9c) ((10a)–(10c), resp.).*

Proof. See Appendix B. □

It follows from Theorem 4 that, in Fig. 4, the periodic solutions arising from the stability boundary loops $(m, 2n)$, $m, n \in \mathbb{Z}$, are of the in-phase mode while those from the loops $(m, 2n + 1)$ the out-of-phase mode.

In Ref. 13, an algebraic condition was given to distinguish an in-phase oscillation from an out-of-phase oscillation. In our investigation, we describe how in-phase and out-of-phase oscillations are related to the stability boundary curves in the (τ_1, τ_2) plane. Therefore, we consider the oscillations from a geometrical point of view which is different from that of Ref. 13.

Next, we derive an analytical expression for a periodic solution arising from Hopf bifurcation using the integration method described in Ref. 36.

Theorem 5. *If $w(t)$ is a periodic solution of the adjoint equation of (26) which is given by*

$$\ddot{w} + \mu\dot{w} + w + \alpha(w_{-\tau_{10}} - Jw_{-\tau_2}) - \beta(\dot{w}_{-\tau_{10}} - J\dot{w}_{-\tau_2}) = 0, \tag{27}$$

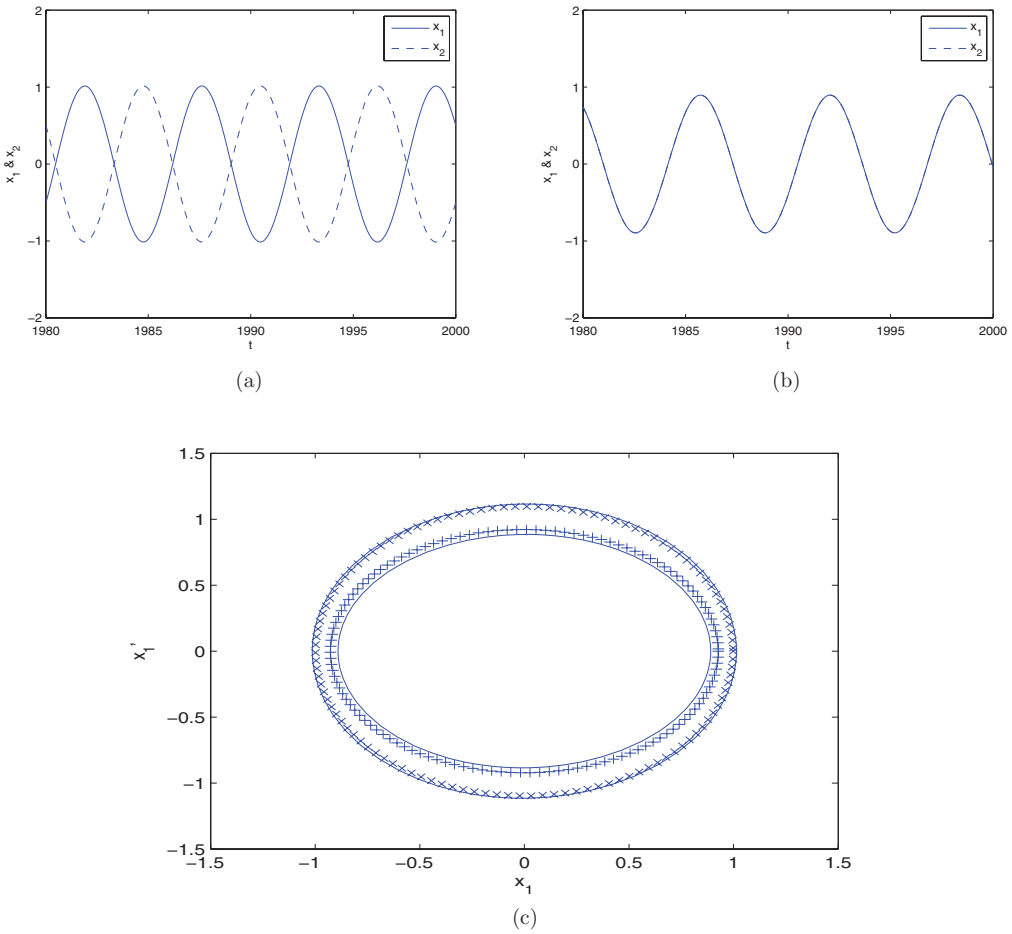

FIG. 8. Time history of the oscillators x_1 (solid) and x_2 (dashed) in (a) the out-of-phase mode and (b) the in-phase mode at $\tau_1 = 1$. (c) A comparison of the zero-order out-of-phase (cross) and in-phase (plus) analytical solutions of (29a) with those from numerical simulations in the phase plane of x_1.

and $w(t) = w(t + 2\pi/\omega)$, *then*

$$
\begin{aligned}
&[w(0)]^T[\dot{z}(2\pi/\omega) - \dot{z}(0)] - [\dot{w}(0)]^T[z(2\pi/\omega) - z(0)] - \mu[w(0)]^T[z(2\pi/\omega) - z(0)] \\
&+ \alpha \int_{-\tau_{10}}^{0} w_{-\tau_{10}}^T[z(t) - z(t + 2\pi/\omega)]dt - \alpha \int_{-\tau_2}^{0} w_{-\tau_2}^T J[z(t) - z(t + 2\pi/\omega)]dt \\
&+ \beta[w(0)]^T\{[z_{\tau_{10}}(2\pi/\omega) - z_{\tau_{10}}(0)] - J[z_{\tau_2}(2\pi/\omega) - z_{\tau_2}(0)]\} \\
&- \beta \int_{-\tau_{10}}^{0} \dot{w}_{-\tau_{10}}^T[z(t) - z(t + 2\pi/\omega)]dt + \beta \int_{-\tau_2}^{0} \dot{w}_{-\tau_2}^T J[z(t) - z(t + 2\pi/\omega)]dt = \epsilon \int_0^{2\pi/\omega} w^T f dt.
\end{aligned}
\tag{28}
$$

Proof. Eq.(28) can be obtained by multiplying both sides of (26) by w^T, integrating with respective to t from 0 to the period $2\pi/\omega$ and applying integration by part. □

Based on the expression of (B1), a periodic solution of (26) for small ϵ can be considered to be a perturbation to (B1) as

$$z_\epsilon(t) = \boldsymbol{p}(\epsilon)\cos(\omega t)K, \tag{29a}$$

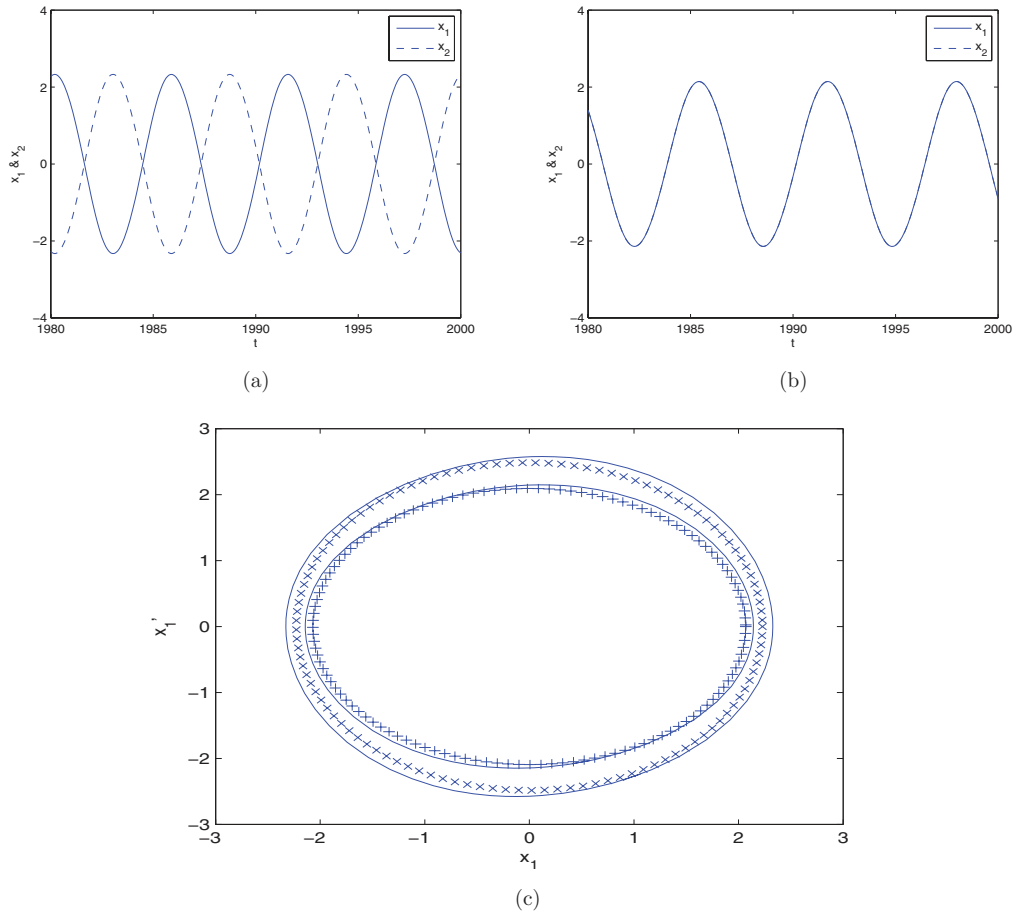

FIG. 9. Time history of the oscillators x_1 (solid) and x_2 (dashed) in (a) the out-of-phase mode and (b) the in-phase mode at $\tau_1 = 1.5$. (c) A comparison of the zero-order out-of-phase (cross) and in-phase (plus) analytical solutions of (29a) with those from numerical simulations in the phase plane of x_1.

where

$$\boldsymbol{p}(\epsilon) = \sum_{i=0}^{\infty} p_i \epsilon^i, \omega = \sum_{i=0}^{\infty} \omega_i \epsilon^i \text{ and } K = \begin{cases} (1,1)^T & \text{for the in-phase mode,} \\ (1,-1)^T & \text{for the out-of-phase mode.} \end{cases} \tag{29b}$$

An analytical expression for the zero-order amplitude p_0 in (29b) can easily be obtained from Theorem 5.

Now, a periodic solution of (27) can be expressed as

$$w(t) = (q_1 \cos(\omega_0 t) + q_2 \sin(\omega_0 t))K, \tag{30}$$

where q_1 and q_2 are independent constants and K is defined in (29b). Substituting (29a)-(29b) and (30) into (28), comparing coefficients of the ϵ term and noting the independence of q_1 and q_2, we obtain two equations in p_0 and ω_1. On solving the equations, we obtain the analytical expressions of p_0 and ω_1 as shown in Corollary 1.

Corollary 1. *Given the system parameters α, β and μ, we assume that ω_0, τ_{10} and τ_2 satisfy either (9a)-(9c) or (10a)-(10c). If a periodic solution of (26) arises from a Hopf bifurcation where τ_{10} is perturbed to $\tau_{10} + \epsilon\tau_{11}$, then ω_1 and p_0 in (29b) are given by*

$$\omega_1 = \frac{\tau_{11}\omega_0[\alpha \sin(\omega_0\tau_{10}) - \beta\omega_0 \cos(\omega_0\tau_{10})]}{\omega_0(\mu\tau_2 - 2) + [\beta\omega_0 \cos(\omega_0\tau_{10}) - \alpha \sin(\omega_0\tau_{10})](\tau_{10} - \tau_2) + \beta S},$$

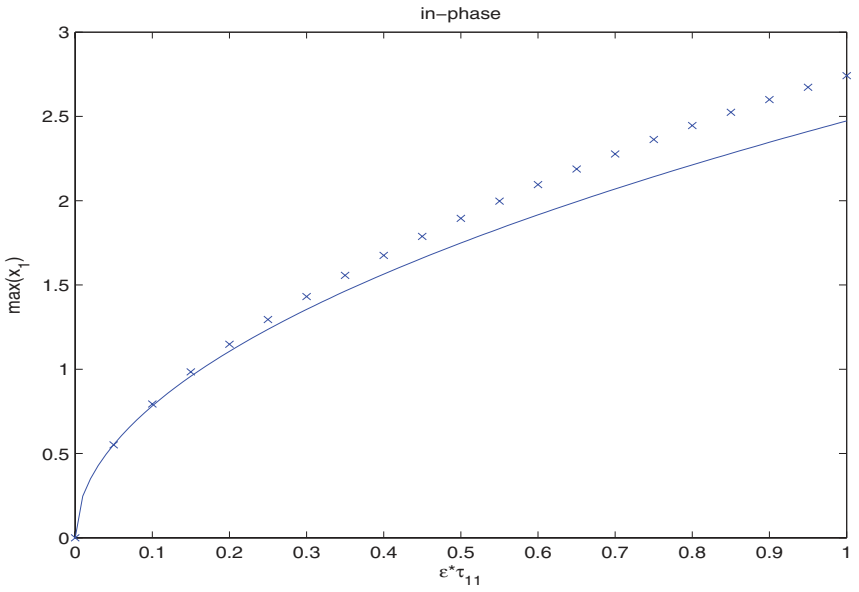

(a)

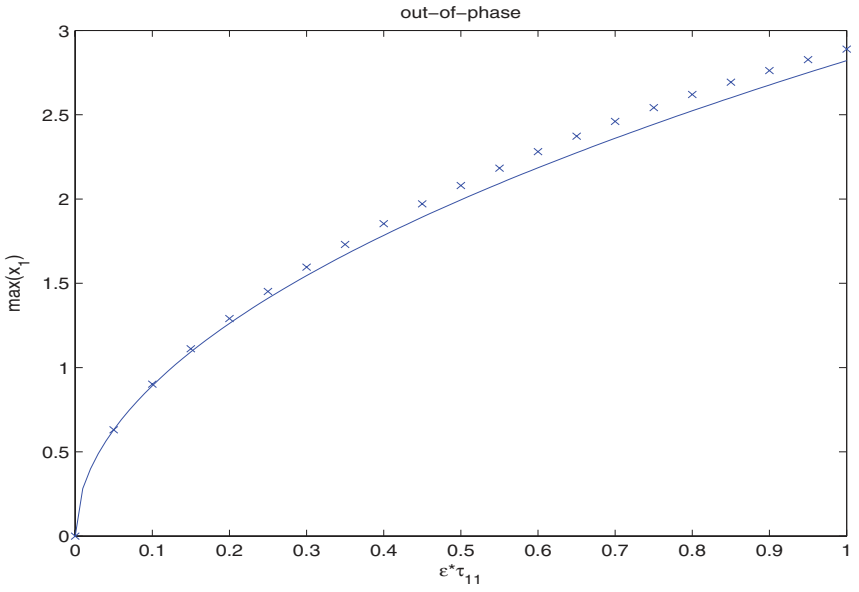

(b)

FIG. 10. A comparison between the zero-order approximate solution (29a) (solid) and the numerical simulation (cross) in Max(x_1) vs. $\epsilon\tau_{11}$ for the periodic solution of system (1) when τ_1 is increased from τ_{10} to $\tau_{10}+1$ (correspondingly $\epsilon\tau_{11}$ from 0 to 1), where (a) the in-phase mode, (b) the out-of-phase mode.

$$p_0 = \frac{2}{\omega_0\sqrt{\mu}}\sqrt{\omega_1\omega_0\tau_2(\omega_0^2-1)+\omega_0[\beta\omega_0\sin(\omega_0\tau_{10})+\alpha\cos(\omega_0\tau_{10})][\omega_1(\tau_{10}-\tau_2)+\omega_0\tau_{11}]-\omega_1\alpha S}$$

where

$$S=\frac{\omega_0(\beta\omega_0^2-\mu\alpha-\beta)}{\beta^2\omega_0^2+\alpha^2}.$$

The stability of a periodic solution arising from a Hopf bifurcation can be determined from the Floquet theory described in Ref. 36.

VI. NUMERICAL SIMULATION

In this section, we perform numerical simulations to illustrate the results obtained from previous sections. In particular, we consider the periodic solutions arising from Hopf bifurcation near the shaded death region shown in Fig. 4 where $(\mu, k, \beta) = (0.05, 0.05, 0.1)$. Let (τ_1, τ_2) be the intersection point of the stability boundary loops (0, 0) and (0, 1). Since it satisfies both (9a)-(9c) and (10a)-(10c), we have $(\tau_1, \tau_2) = (0.8744, 1.4249)$. From Theorem 4, if τ_1 is increased from $\tau_{10} = 0.8744$ while keeping τ_2 unchanged at 1.4249, we would expect a stable periodic solution of the in-phase mode arising from a Hopf bifurcation out of the stability boundary loop (0, 0) and another stable periodic solution of the out-of-phase mode from the loop (0, 1). As predicted from theoretical consideration, we find two periodic solutions as τ_1 is increased from τ_{10}. Figures 8(a) and 8(b) show the numerical simulation in time history for the in-phase mode and out-of-phase mode, respectively, at $\tau_1 = 1$. A comparison of the phase portraits between the analytical solutions obtained from Corollary 1 and numerical simulations is depicted in Fig. 8(c). Figures 9(a)-9(c) show the periodic solutions at $\tau_1 = 1.5$. In Fig. 10, the periodic solutions obtained from Corollary 1 are compared with those obtained from numerical simulation as τ_1 is increased. It can be seen that they are in good agreement.

VII. CONCLUSIONS

In this paper, we perform a stability analysis of a pair of van der Pol oscillators with delayed self-connection, position and velocity couplings. By introducing a parameter γ where $0 < \gamma \leq 1$ in the local stability analysis, stability boundary curves can easily be obtained if they exist. Bifurcation diagram on stability analysis of the damping, position and velocity coupling strengths is constructed, which consists of three types of regions: (i) absolutely unstable region, (ii) regions where closed stability boundary curves exist, and (iii) regions where the stability boundary curves are open-ended. Stability switching regions are observed near the τ_2-axis. An interesting question arises naturally: for arbitrary large damping strength μ, can the zero equilibrium of a pair of van der Pol oscillators be stabilized using the delayed position and velocity couplings strategy? Theorem 3 gives an affirmative answer. A sufficient condition which requires only one time delay τ_2 is found for the stabilization of the zero equilibrium. With delayed velocity coupling alone, it was shown in Ref. 16 that stabilization of the zero equilibrium can be achieved when $\mu < 0.5$. However, with both delayed position and velocity couplings, it is shown that stability of the zero equilibrium can be achieved for arbitrary large μ. A general question arises naturally, for a network of van der Pol oscillators with any topological connection, is it possible to derive a delayed couplings strategy to stabilize the zero equilibrium for arbitrary large damping strength μ? The question will be dealt with in future.

Periodic solutions of the in-phase and the out-of-phase modes coexist in system (1). We have shown how the type of mode is related to the stability boundary curve that a periodic solution emerges from a Hopf bifurcation. The amplitude of a periodic solution can easily be obtained using an integration method. The analytical solutions agree very well with those from numerical simulation.

ACKNOWLEDGMENT

This work was supported by the Hong Kong Research Grant Council under CERG Grant (CityU 1005/07E). The constructive comments by the anonymous reviewers are gratefully acknowledged.

APPENDIX A

Proof of Theorem 1: Since a positive solution of (9a) is 1 equivalent to a pair of purely imaginary roots of (3a), we only need to prove that the region specified by the inequalities in each part of Lemma 3 or Lemma 4 corresponds to one of the regions defined in this theorem.

From the definition of γ_+ in (11b) and $\gamma_{1,2}$ in (12), we have

$$\gamma_+^2 = 1 \quad \Leftrightarrow \beta^2 = \frac{1}{2}\left[\frac{\mu^2}{2} - 1 - k^2 + \sqrt{(1+k^2)^2 - \mu^2 k^2}\right],$$

$$\gamma_1 = 1 \quad \Leftrightarrow |\beta| = \frac{1}{2|k|} \text{ and } \gamma_2^2 = 1 \Leftrightarrow \mu^2 = 4\beta^2 + 2.$$

Fig. 3(b) shows the curves of $\gamma_i^2 = 1$ for $i \in \{+, 1, 2\}$ and the regions where γ_i^2 is greater or less than one. These curves intersect concurrently at two points

$$P_\pm = \left(\sqrt{2 + \frac{1}{k^2}}, \pm\frac{1}{2|k|}\right).$$

The region specified by the inequalities of Lemma 3(a) is given by

$$\gamma_1 > 1 \quad \text{and} \quad (\gamma_2^2 \geq 1 \quad \text{or} \quad \gamma_+ > 1)$$
$$\Longleftrightarrow |\beta| > \frac{1}{2|k|} \quad \text{and} \quad \left(\mu^2 \geq 4\beta^2 + 2 \quad \text{or} \quad \beta^2 > \frac{1}{2}\left[\frac{\mu^2}{2} - 1 - k^2 + \sqrt{(1+k^2)^2 - \mu^2 k^2}\right]\right).$$

It can be shown easily that the points satisfying the above inequalities are those to the right of the curves OP_+ and OP_- in Fig. 3(b) (see the shaded area), i.e. the points in region *I* defined in this theorem (see Fig. 3). From Lemma 3(a), since (9a) has no positive solution for this set of points, (3a) has no purely imaginary root. This proves part (a). Furthermore, the region specified by the inequalities of Lemma 3(b) corresponds to region *II*. Finally, since

$$\gamma_1^2 \leq \gamma_2^2 \Leftrightarrow \mu \geq \sqrt{2 + \frac{1}{k^2}},$$

the regions specified by the inequalities of Lemma 4(a) and 4(b) correspond to regions III_a and III_b, respectively. This completes the proof.

APPENDIX B

Proof of Theorem 4: Assume that at the Hopf bifurcation, a pair of eigenvalues in (3a) cross the imaginary axis at $\lambda = \pm i\omega_0$. Then, for $|\epsilon| \ll 1$, the zero-order periodic solution of (26) can be expressed as

$$z_0 = \boldsymbol{p}\cos(\omega_0 t) + \boldsymbol{q}\sin(\omega_0 t), \tag{B1}$$

where $\boldsymbol{p} = (p_1, p_2)^T, \boldsymbol{q} = (q_1, q_2)^T$. Substituting (B1) into (26) yields

$$M\boldsymbol{p} = -N\boldsymbol{q} \quad \text{and} \quad M\boldsymbol{q} = N\boldsymbol{p}, \tag{B2}$$

where $M = \begin{pmatrix} m_1 & m_2 \\ m_2 & m_1 \end{pmatrix}$, $N = \begin{pmatrix} n_1 & n_2 \\ n_2 & n_1 \end{pmatrix}$ and

$$\begin{cases} m_1 = -\omega_0^2 + 1 + \beta\omega_0 \sin(\omega_0\tau_{10}) + \alpha\cos(\omega_0\tau_{10}), \\ m_2 = -\beta\omega_0 \sin(\omega_0\tau_2) - \alpha\cos(\omega_0\tau_2), \\ n_1 = -\mu\omega_0 + \beta\omega_0\cos(\omega_0\tau_{10}) - \alpha\sin(\omega_0\tau_{10}), \\ n_2 = -\beta\omega_0\cos(\omega_0\tau_2) + \alpha\sin(\omega_0\tau_2). \end{cases}$$

If the Hopf bifurcation comes from a stability boundary curve generated by (9a)-(9c), it follows from (4a) that $m_1 = -m_2$ and $n_1 = -n_2$ and so, from (B2), $p_1 = p_2$ and $q_1 = q_2$. Therefore, the periodic solution is of the in-phase mode. On the other hand, if the Hopf bifurcation is from a curve generated by (10a)-(10c), we have from (4b) that $m_1 = m_2$ and $n_1 = n_2$ which imply $p_1 = -p_2$ and $q_1 = -q_2$. The periodic solution is of the out-of-phase mode.

[1] P. M. Varangis, A. Gavrielides, T. Erneux, V. Kovanis, and L. F. Lester, "Frequency entrainment in optically injected semiconductor lasers," Phys. Rev. Lett. **78**, 2353–2356 (1997).
[2] A. Hohl, A. Gavrielides, T. Erneux, and V. Kovanis, "Localized synchronization in two coupled nonidentical semiconductor lasers," Phys. Rev. Lett. **78**, 4745–4748 (1997).
[3] I. Schreiber and M. Marek, "Strange attractors in coupled reaction diffusion cells," Phys. D **5**, 258–272 (1982).
[4] M. Dolnik and I. R. Epstein, "Coupled chaotic chemical oscillators," Phys. Rev. E **54**, 3361–3368 (1996).

[5] M. Kawato and R. Suzuki, "Two coupled neural oscillators as a model of the circadian pacemaker," J. Theoret. Biol. **86**, 547–575 (1980).
[6] J. Wei and M. Y. Li, "Global existence of periodic solutions in a tri-neuron network model with delays," Phys. D **198**, 106–119 (2004).
[7] S. A. Campbell, R. Edwards, and P. van den Driessche, "Delayed coupling between two neural network loops," SIAM J. Appl. Math. **65**, 316–335 (2004).
[8] S. A. Campbell, I. Ncube, and J. Wu, "Multistability and stable asynchronous periodic oscillations in a multiple-delayed neural system," Phys. D **214**, 101–119 (2006).
[9] F. M. Atay, "Delay-induced stability: from oscillators to networks," in *Complex Time-Delay Systems, Underst. Complex Syst.* (Springer, Berlin, 2010) pp. 45–62.
[10] F. M. Atay, "Van der Pol's oscillator under delayed feedback," J. Sound Vibration **218**, 333–339 (1998).
[11] A. Maccari, "The response of a parametrically excited van der Pol oscillator to a time delay state feedback," Nonlinear Dynam. **26**, 105–119 (2001).
[12] J. Xu and K. W. Chung, "Effects of time delayed position feedback on a van der Pol-Duffing oscillator," Phys. D **180**, 17–39 (2003).
[13] S. Wirkus and R. Rand, "The dynamics of two coupled van der Pol oscillators with delay coupling," Nonlinear Dynam. **30**, 205–221 (2002).
[14] X. Li, J. C. Ji, and C. Hansen, "Dynamics of two delay coupled van der Pol oscillators," Mechanics Research Communications **33**, 614–627 (2006).
[15] J. M. Zhang and X. S. Gu, "Stability and bifurcation analysis in the delay-coulped van der Pol oscillators," Appl. Math. Model. **34**, 2291–2299 (2010).
[16] Y. L. Song, "Hopf bifurcation and spatio-temporal patterns in delay-coupled van der Pol oscillators," Nonlinear Dynam. **63**, 223–237 (2011).
[17] K. Bar-Eli, "On the stability of coupled chemical oscillators," Phys. D **14**, 242–252 (1985).
[18] D. G. Aronson, G. B. Ermentrout, and N. Kopell, "Amplitude response of coupled oscillators," Phys. D **41**, 403–449 (1990).
[19] M. Y. Kim, R. Roy, J. L. Aron, T. W. Carr, and I. B. Schwartz, "Scaling Behavior of Laser Population Dynamics with Time-Delayed Coupling: Theory and Experiment," Phys. Rev. Lett. **94**, 088101 (2005).
[20] P. Kumar, A. Prasad, and R. Ghosh, "Stable phase-locking of an external-cavity diode laser subjected to external optical injection," J. Phys. B **41**, 135402 (2008).
[21] M. Rosenblum and A. Pikovsky, "Delayed feedback control of collective synchrony: An approach to suppression of pathological brain rhythms," Phys. Rev. E **70**, 041904 (2004).
[22] A. Schnitzler and J. Gross, "Normal and pathological oscillatory communication in the brain," Nat. Rev. Neurosci **6**, 285–296 (2005).
[23] D. J. Selkoe, "Toward a comprehensive theory for Alzheimer's disease. Hypothesis: Alzheimer's disease is caused by the cerebral accumulation and cytotoxicity of amyloid beta-protein," Ann. N. Y. Acad. Sci. **924**, 17–25 (2000).
[24] R. E. Tanzi, "The synaptic Abold beta hypothesis of Alzheimer disease," Nat Neurosci. **8**, 977–979 (2005).
[25] B. Caughey and P. T. Lansbury, "Protofibrils, pores, fibrils, and neurodegeneration: separating the responsible protein aggregates from the innocent bystanders," Annu. Rev. Neurosci. **26**, 267–298 (2003).
[26] A. Koseska and E. Volkov, "Parameter mismatches and oscillation death in coupled oscillators," Chaos **20**, 023132 (2010).
[27] D. V. Reddy, A. Sen, and G. L. Johnston, "Time delay induced death in coupled limit cycle oscillators," Phys. Rev. Lett. **80**, 5109–5112 (1998).
[28] K. Konishi, "Amplitude death induced by dynamic coupling," Phys. Rev. E **68**, 067202 (2003).
[29] R. Karnatak, R. Ramaswamy, and A. Prasad, "Amplitude death in the absence of time delays in identical coupled oscillators," Phys. Rev. E **76**, 035201 (2007).
[30] D. V. Reddy, A. Sen, and G. L. Johnston, "Time delay effects on coupled limit cycle oscillators at Hopf bifurcation," Phys. D **129**, 15–34 (1999).
[31] Y. Song, J. Wei, and Y. Yuan, "Stability switches and Hopf bifurcations in a pair of delay-coupled oscillators," J. Nonlinear. Sci. **17**, 145–166 (2007).
[32] K. Pyragas, "Continuous control of chaos by self-controlling feedback," Phys. Lett. A **170**, 421–428 (1992).
[33] A. Ahlborn and U. Parlitz, "Stabilizing Unstable Steady States Using Multiple Delay Feedback Control," Phys. Rev. Lett. **93**, 264101 (2004).
[34] A. Ahlborn and U. Parlitz, "Controlling dynamical systems using multiple delay feedback control," Phys. Rev. E **72**, 016206 (2005).
[35] K. B. Blyuss, Y. N. Kyrychko, P. Hvel, and E. Schll, "Control of unstable steady states in neutral time-delayed systems," Eur. Phys. J. B. **65**, 571–576 (2008).
[36] J. Xu, K. W. Chung, and C. L. Chan, "An efficient method for studying weak resonant double Hopf bifurcation in nonlinear systems with delayed feedbacks," SIAM J. Appl. Dyn. Syst. **6**, 29–60 (2007).
[37] A. Sen, R. Dodla, G. L. Johnston, and G. C. Sethia, "Amplitude death, synchrony, and chimera states in delay coupled limit cycle oscillators," in *Complex time-delay systems, Underst. Complex Syst.* (Springer, Berlin, 2010) pp. 1–43.
[38] K. W. Chung, C. L. Chan, and J. Xu, "An Efficient Method for Switching Branches of Period-doubling Bifurcations of Strongly Non-linear Autonomous Oscillators with Many Degrees of Freedom," Journal of Sound and Vibration **267**, 787–808 (2003).
[39] K. Gu, N.-I. Niculescu, and J. Chen, "On stability crossing curves for general systems with two delays," J. Math. Anal. Appl. **311**, 231–253 (2005).